International Journal of Biochemistry and Cell Biology 117 (2019) 105639

Contents lists available at ScienceDirect

International Journal of Biochemistry and Cell Biology

journal homepage: www.elsevier.com/locate/biocel

The effect of core fucosylation-mediated regulation of multiple signaling pathways on lung pericyte activation and fibrosis

Ying Sun[a,1], Wei Sun[d,1], Ning Yang[c], Jia Liu[b], HaiYing Tang[b], Fengzhou Li[b], Xiuna Sun[b], Lili Gao[b], Fuyang Pei[a], Jia Liu[c], Hongli Lin[c,**], Wu Taihua[b,*]

[a] Departments of Respiratory Medicine, The Affiliated Zhongshan Hospital of Dalian University, Dalian, Liaoning 116001, PR China
[b] Departments of Respiratory Medicine, The First Affiliated Hospital of Dalian Medical University, Dalian, Liaoning 116011, PR China
[c] Departments of Nephrology, The First Affiliated Hospital of Dalian Medical University, Dalian, Liaoning 116011, PR China
[d] Post-doctoral research station, Peking Union Medical College Hospital, Chinese Academy of Medical Science & Peking Union Medical College, Beijing 100730, PR China

ARTICLE INFO

Keywords:
Pulmonary fibrosis
Pericytes
Myofibroblasts
FUT8

ABSTRACT

The main event in the progression of pulmonary fibrosis is the appearance of myofibroblasts. Recent evidence supports pericytes as a major source of myofibroblasts. TGFβ/Smad2/3 and PDGF/Erk signaling pathways are important for regulating pericyte activation. Previous studies have demonstrated that PDGFβR and TGFβR are modified by core fucosylation (CF) catalyzed by α-1,6-fucosyltransferase (FUT8). The aim of this study was to compare the effect of inhibiting CF versus the PDGFβR and TGFβR signaling pathways on pericyte activation and lung fibrosis. FUT8shRNA was used to knock down FUT8-mediated CF both in vivo and in isolated lung pericytes. The small molecule receptor antagonists, ST1571 (imatinib) and LY2109761, were used to block the PDGFβ/pErk and TGFβ/pSmad2/3 signaling pathways, respectively. Pericyte detachment and myofibroblastic transformation were assessed by immunofluorescence and Western blot. Histochemical and immunohistochemical staining were used to evaluate the effect of the intervention on pulmonary fibrosis. Our findings demonstrate that FUT8shRNA significantly blocked pericyte activation and the progression of pulmonary fibrosis, achieving intervention effects superior to the small molecule inhibitors. The PDGFβ and TGFβ pathways were simultaneously affected by the CF blockade. FUT8 expression was upregulated with the transformation of pericytes into myofibroblasts, and silencing FUT8 expression inhibited this transformation. In addition, there is a causal relationship between CF modification catalyzed by FUT8 and pulmonary fibrosis. Our findings suggest that FUT8 may be a novel therapeutic target for pulmonary fibrosis.

1. Introduction

The number of patients with pulmonary fibrosis continues to steadily increase, and the absence of an effective therapy has led to heavy economical and public health burdens throughout the world (Sköld et al., 2019; Lunardi et al., 2018; Feng et al., 2019). Activation of myofibroblasts and the production of an abundance of extracellular matrix (ECM) is the pathophysiological mechanism of pulmonary fibrosis (Urushiyama et al., 2019 ; Shao et al., 2018). Moreover, ECM has been found to increase lung ischemia and hypoxia, which further promotes pulmonary fibrosis (Kathiriya et al., 2017 ; Braun et al., 2018 ; Terashima et al., 2019).

Recent studies have demonstrated that pericytes, which regulate microvascular circulation and physiological function may be an important source of myofibroblasts (Wang et al., 2019a, 2019b ; Sava et al., 2017 ; Kumar et al., 2017 ; Wang et al., 2017). The mechanism of pulmonary fibrosis involves pericyte transdifferentiation into myofibroblasts through the TGF-β/Smad2/3 and PDGFβ/Erk signaling pathways (Underly et al., 2017; Hirooka et al., 2017 ; Pozdzik et al., 2016; Castellano et al., 2019 ; Minutti et al., 2019). Thus, the blockade

Abbreviations: CF, core fucosylation; FUT8, α-1,6-fucosyltransferase; TGFβ, transforming groth factor-β; TGFβR, transforming groth factor-β receptor; PDGFβ, platelet derived growth factor-β; PDGFβ, platelet derived growth factor-β receptor; ECM, extracellular matrix; α-SMA, α-Smooth Muscle Actin; BLM, bleomycin

* Corresponding author at: Departments of Respiratory Medicine, The First Affiliated Hospital of Dalian Medical University, 222# Zhongshan Road, Dalian, Liaoning 116011, PR China.
** Corresponding author at: Departments of Nephrology, The First Affiliated Hospital of Dalian Medical University, 222# Zhongshan Road, Dalian, Liaoning, 116011, PR China.
E-mail addresses: linhonglidoc@126.com (H. Lin), wutaihuadoc@126.com (W. Taihua).
[1] These authors have contributed to this work and shares the first authorship.

https://doi.org/10.1016/j.biocel.2019.105639
Received 12 August 2019; Received in revised form 20 October 2019; Accepted 21 October 2019
Available online 24 October 2019
1357-2725/

of a single signaling pathway may not significantly inhibit pericyte activation. Previous studies have reported that the key receptors (TGFβR and PDGFβR) are modified by α-1,6-core fucosylation (CF) catalyzed by fucosyltransferase8 (FUT8) (Sun et al., 2017). CF modification catalyzed by FUT8 is an important method of modified glycosylation (Chen et al., 2016; Shen et al., 2013; Hirano et al., 2017). However, CF modification in pulmonary fibrosis remains unknown. Therefore, we hypothesize that inhibition of CF modification of TGFβR and PDGFβR can block pericyte activation and thus alleviate pulmonary fibrosis.

To test our hypothesis, we established a bleomycin-induced murine model of pulmonary fibrosis and an adenovirus-encapsulated *FUT8*shRNA was used to knockdown C57BL/6 mice (CF modification of many key proteins in the mouse lungs are inhibited). The small-molecule receptor antagonists, imatinib (PDGFβR) and LY2109761 (TGFβR), were given to block the PDGFβ/pErk and TGF-β/pSmad2/3 signaling pathways, respectively as the single signal pathway inhibition groups. The migration of pericytes and the effect on the transdifferentiation of pericytes into myofibroblasts were compared. Finally, the effect of each intervention on pulmonary pathology and ECM between the multi-pathway group and single pathway groups were compared to further clarify the impact of CF modification on pericyte activation in the progression of pulmonary fibrosis.

2. Materials and methods

2.1. Care and use of laboratory animals

All experimental protocols were reviewed and approved by the Committee on Ethics of Animal Experimentation of Dalian Medical University. Animal experiments were conducted in accordance with the regulations set by the institutional committee for the care and use of laboratory animals, and approved by local authorities. Male C57BL/6 J mice (age: 8 weeks; weight: 17 g–22 g; obtained from Dalian Medical University) were housed in a 12 h light/dark cycle, and were provided free access to food and water.

2.2. Reagents

Bleomycin (BLM; 15 mg/per mouse) was produced by Nippon Kayaku Co., Ltd. (batch number: 450260). Imatinib mesylate (ST1571) was provided by Novartis Pharmaceutical Co., Ltd. (Beijing, China). LY2109761 was purchased from Selleck Co. (United States). The *FUT8*shRNA recombinant adenovirus was purchased from Wuhan Genesil Biotechnology Co., Ltd. (Wuhan, China)

2.3. BLM mouse model of pulmonary fibrosis

The mice were anesthetized with 4% chloral hydrate (0.1 mL/10 g body weight) via an intraperitoneal injection. Following local disinfection, the throat of each mouse was cut to expose the trachea via blunt dissection. The BLM solution was injected quickly from the trachea using a 1 mL injector. The mice were placed vertically and turned three to four times. Finally, the wound was sutured and the mice awakened naturally.

2.4. Administration of STI571, LY2109761, and FUT8shRNA intervention in animals

Mice in the different groups were gavaged with STI571 and LY2109761 (100 mg/day/kg) 24 h after BLM administration for three weeks. The adenovirus-encapsulated FUT8shRNA (5′ GCUACUGAUGA UCCUACUU dTdT 3′; 3′ dTdT CGAUGACUACUAGGAUGAA 5′) was injected into the tail vein to establish a systemic infection one day after BLM administration (1 × 106 PFU of Ad-FUT8shRNA [Genepharma]). The mice were sacrificed on the 28th day and the lungs were collected.

2.5. Plasmids and lentivirus

shRNA fragments targeting the FUT8 gene, one expression clone fragment encoding the full length of the FUT8 ORF sequence and the corresponding negative control fragments were purchased from Genepharma. Lentiviral particles were generated by following a standardized protocol using highly purified plasmids and EndoFectin-Lenti and TiterBoost reagents. Cell transfection was conducted according to our previous reports (Sun et al., 2017).

2.6. Pericyte isolation and culture

All experiments were performed in accordance with the Research Ethics Committees of DaLian Medical University, China. We isolated primary pericytes from C57BL/6 J mice. Briefly, the fresh lung tissue was washed three times with Hanks' balanced salt solution; the lung tissues were removed and cut into 0.5 x 0.5 mm small pieces, and the lung tissues were digested with liberate TM (Roche Applied Science) for approximately 50 min at 37 °C on an orbital shaker. The digested lung tissue was filtered through a 100 μm and 200 μm nylon mesh (Falcon, BD, US). Mouse lung cells were collected in a 50 mL centrifuge tube and centrifuged. We added 4 μL rabbit anti- PDGFβR monoclonal antibody (ab93563, Abcam, US) for 15 min at 4 °C. Then, the lung pericytes were suspended in 320 μL D-Hanks balanced salt solution and incubated in 80 μL anti-mouse IgG beads (Miltenyi Biotec) for 15 min at 4 °C. After washing three times, the bead-bound pericytes were seeded into gelatin-coated cell culture plates containing the pericyte medium (ScienCell, US).

2.7. Animal model of STI571, LY2109761, and FUT8shRNA stimulation of the transformed pericytes via interfering TGFβ1

The normal pericytes were cultured in pericyte medium. The in vitro pericyte transformation model was established after incubating the pericytes in TGF-β1 (5 ng/mL) for 72 h. Next, STI571 (10 μmol/L) and LY2109761 (2 μmol/L) were added as intervetion. Chemically synthesized FUT8-shRNAs were designed to target the FUT8 gene. The shRNA sequence was identified using the mouse genome database to assess any potential cross-reactivity. After synthesis, 20 nM FUT8shRNA (5′ GCUACUGAUGAUCCUACUU dTdT 3′; 3′ dTdT CGAUGACUACUAG GAUGAA 5′) and TGF-β1 (5 ng/mL) were incubated with the pericytes. The pericytes in these intervention groups were observed for transformation at different time points.

2.8. Western blotting

The protein concentration of the whole lysates was determined using BCA protein assay kits (Pierce Biotechnology, Rockford, IL). Protein samples were heated to 100 °C for 5 min, and 20 mL aliquots were separated via sodium dodecyl sulfate-polyacrylamide gel electrophoresis and transferred to polyvinylidene difluoride membranes. The membranes were incubated with primary antibodies against FUT8, α-SMA, p-Erk, or p-Smad2/3 (1:200; Abcam, US) in 10 mL dilution buffer (1 Tris-buffered saline, 0.1% Tween-20 with 5% bovine serum albumin), with agitation overnight at 4 °C. The membranes were then incubated with the appropriate horseradish peroxidase–conjugated secondary antibody (1:5000; Zhongshan Biotechnology, Beijing, China) in 10 mL dilution buffer with agitation for 1 h at 25 °C. Bands were detected using an ECL kit (Amersham) and protein expression was quantified using Labworks Image Analysis software (UVP, Upland, CA).

2.9. Double immunofluorescent analysis

Frozen lung sections (5 μm) were incubated overnight with the primary anti-PDGFβR antibody, anti-Desmin antibody, anti-α-SMA antibody, anti-FUT8 antibody (1:100; Abcam, US), then incubated with

an TRITC-goat anti-rat antibody and FITC-goat anti-rabbit antibody (1:200; Zhongshan Biotechnology) for 30 min at 25 °C in the dark. After washing three times with PBS for 5 min, the sections were counterstained and mounted as previously described. The slides were viewed and the staining intensity was analyzed as previously described.

2.10. Histological examination

Following sacrifice, the right lungs were removed and fixed in 4% paraformaldehyde, dehydrated, and embedded in paraffin. The paraffin-embedded tissue samples were sectioned into 5 μm slices and stained with Masson's trichrome, and examined under a light microscope (DP73; Olympus). The lung tissues were quantified via morphometric analysis using a light microscope (Carl Zeiss, Thornwood, NY). The quantification of fibrotic areas in the lung fibrotic regions were evaluated via computer-based morphometric analysis (Olympus, Tokyo, Japan).

2.11. Immunohistochemistry

Tissue samples in 5-μm slices were deparaffinized in xylene, hydrated with graded alcohol and then washed with 1% PBS. Subsequently, these slices were first incubated in 10 mmol/L citrate buffer (pH 6.0) at 100 °C for 10 min to retrieve the antigen and then placed in 3% hydrogen peroxide for 15 min at room temperature to block any endogenous peroxidase activity. After rinsing with 1% PBS three times, the sections were blocked with goat serum for 30 min, incubated with a rabbit polyclonal primary anti-timp1 antibody, anti-collagen I antibody, anti-collagen III antibody (1:100, Abcame, US) at 4 °C overnight. Subsequently, the sections were washed with 1% PBS, incubated with the corresponding goat anti-rabbit biotinlabeled secondary antibody (1:200; Beyotime, Shanghai, China) at 37 °C for 30 min and subsequently incubated in an avidinhorseradish peroxidase complex (Beyotime). Proteins were visualized using DAB staining. The lung tissues were quantified via morphometric analysis using a light microscope (Carl Zeiss, Thornwood, NY). Quantification of fibrotic areas and positively stained lung fibrotic regions (brown color) were evaluated by computer-based morphometric analysis (Olympus, Tokyo, Japan).

2.12. Statistical analysis

Data are expressed as the mean ± S.D. values. The statistical analysis was performed using an analysis of variance with a Tukey's *post-hoc* analysis. Statistical significance was set at $P < 0.05$.

3. Results

3.1. TGF-β1 increases the expression of FUT8, PDGFβR, and TGFβR in lung pericytes

We used TGF-β1 stimulated pericytes as a model of pulmonary fibrosis in vivo. Pericytes derived from the lung were sorted using immunomagnetic beads and incubated with TGF-β1 for 48 h. The expression of FUT8, PDGFβR, and TGFβR were labeled with green fluorescence. The results revealed that there was a moderate fluorescence intensity in the lung pericytes. The expression of FUT8, PDGFβR, and TGFβR was significantly increased after the pericytes were incubated with TGF-β1 (48 h), indicating that the expression of key proteins was up-regulated in the process of TGF-β1-induced pericyte transdifferentiation (Fig. 1A and B).

3.2. FUT8shRNA, STI571, and LY2109761 inhibited the expression of endogenous FUT8, PDGFβR, and TGF-βR in BLM models

First, we found that FUT8 expression in the BLM mouse model was upregulated and that FUT8shRNA downregulated FUT8 expression for at least 28 days by Western blot. Second, we sought to determine whether STI571 or LY2109761 can downregulate the expression of PDGFβR and TGFβR in the BLM model. Our results showed that STI571 and LY2109761 can down-regulate the expression of PDGFβR and TGFβR, respectively by Western blot (Fig. 2A and B). These findings indicate that STI571 and LY2109761 inhibit the activation of PDGF/Erk and TGF/Smad2/3 signaling pathways, respectively.

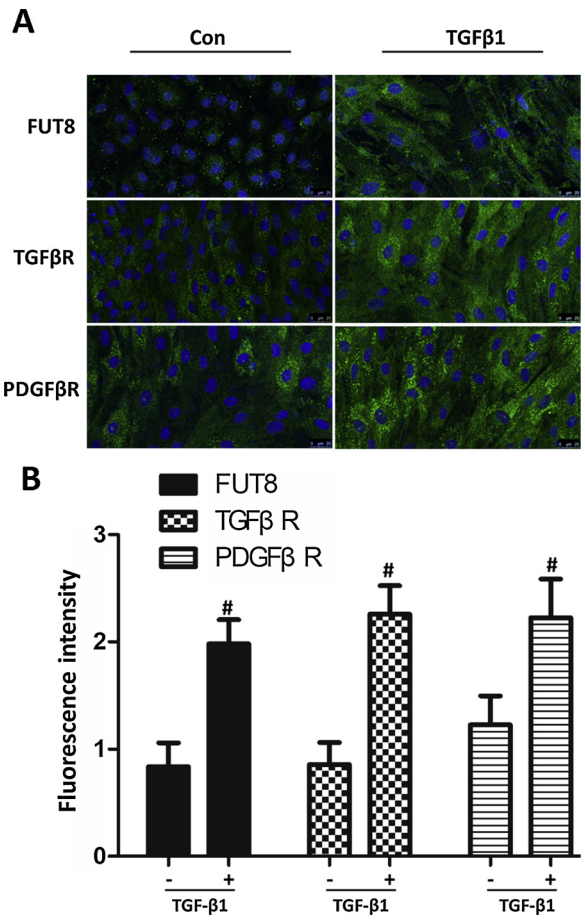

Fig. 1. Upregulated FUT8, PDGFβR, and TGFβR proteins induced by TGF-β1 in pericytes. A: The expression of FUT8, PDGFβR, and TGFβR was detected by immunofluorescence in each group (magnification: × 400). B: Quantitative analysis of immunofluorescence results. Scale bar, 50 μm. All data are expressed as the mean ± S.D. values. TGF-β1 group was compared with the Control group, #$P < 0.01$. Each experiment was repeated three times (n = 6).

3.3. Comparison of the effects of FUT8shRNA, STI571, and LY2109761 on pericyte transition

Pericyte transition is dependent on the activation factors secreted by endothelial cells (Starling, 2017). Two markers (PDGFβR and Desmin) were used to label pericytes in order to detect the effect of different treatments on pericyte transdifferentiation in a BLM model. The in vivo results confirmed that pericyte detachment and transdifferentiation into myofibroblasts from endothelial cells (CD31 +) cannot be completely inhibited following treatment with STI571 and LY2109761. However, effective inhibition was observed in the FUT8shRNA group by both immunofluorescence staining and Western blot analyses (Figs. 3 and 4A).

To verify these results, the lung pericytes were incubated with TGF-β1 for 48 h. We found that myofibroblast-like morphological changes were observed in the pericytes along with increased expression of α-SMA. STI571 and LY2109761 could not inhibit the expression of α-

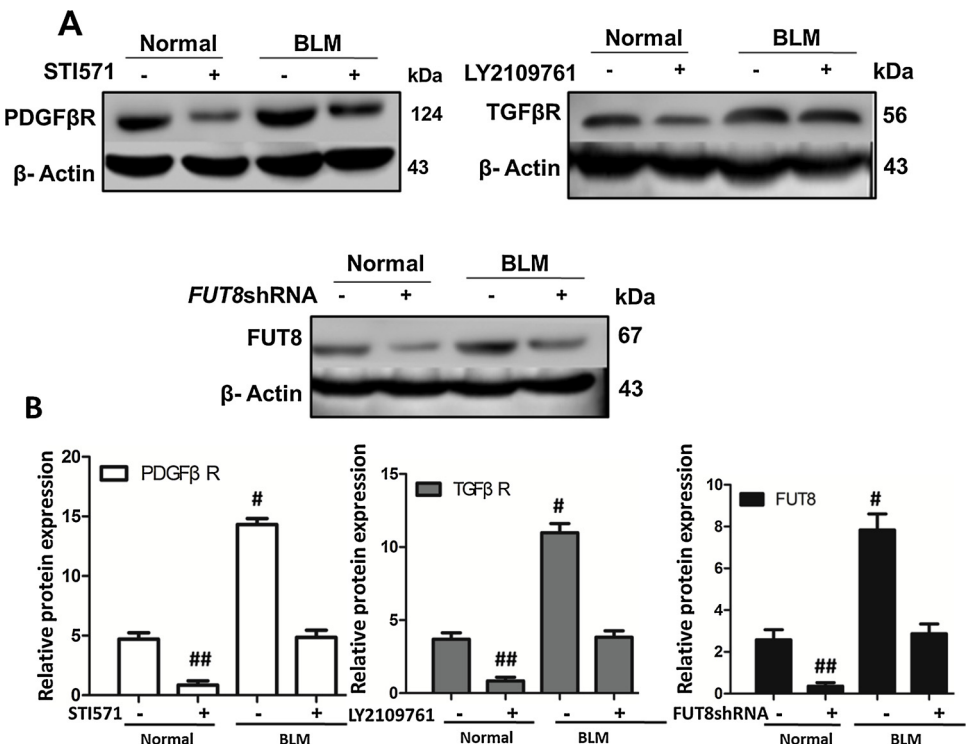

Fig. 2. *FUT8*shRNA, STI571, and LY2109761 inhibited the expression of FUT8, PDGFβR, and TGF-βR, respectively in a BLM model. A: Intervention effect of STI571, and LY2109761, and *FUT8*shRNA by Western blot. B: Quantitative analysis of Western blot. Western blots were performed on the total lung lysate. All data are expressed as the mean ± S.D. values. #P < 0.01 versus the Normal group; ##P < 0.01 versus the BLM group. Each experiment was repeated for three times (n = 6).

SMA, whereas *FUT8*shRNA clearly blocked the expression of α-SMA (Fig. 4B). These results indicate that multiple signaling pathways (PDGFβ/pErk and TGF-β/pSmad2/3) are involved in the transdifferentiation of pericytes into myofibroblasts in the pulmonary mesenchyme. In addition, a blockade of a single signaling pathway does not effectively inhibit pericyte transdifferentiation.

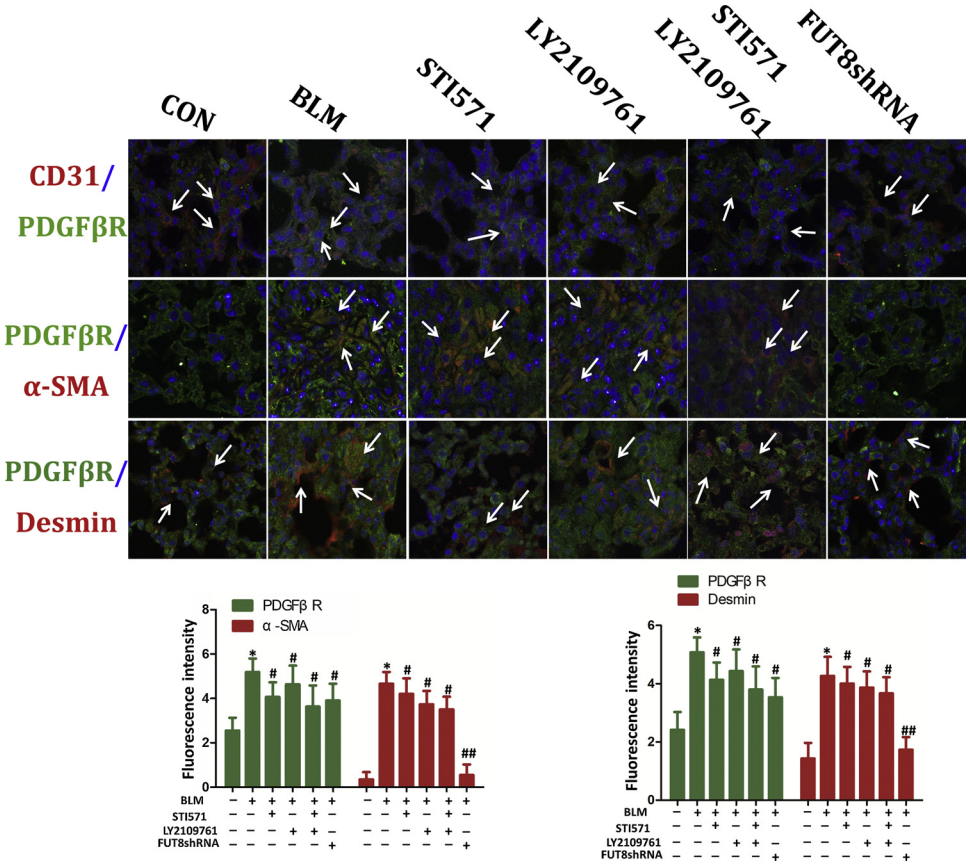

Fig. 3. The effect of *FUT8*shRNA, STI571, and LY2109761 on the pulmonary pericyte-myofibroblast transition. Representative images of PDGFRβ (green) and CD31, α-SMA, Desmin staining (red) and quantitative analysis. White arrows indicate pericytes. *P < 0.01 versus Control group; #P > 0.05 versus BLM group; ##P < 0.01 versus the BLM group. (For interpretation of the references to colour in this figure legend, the reader is referred to the web version of this article).

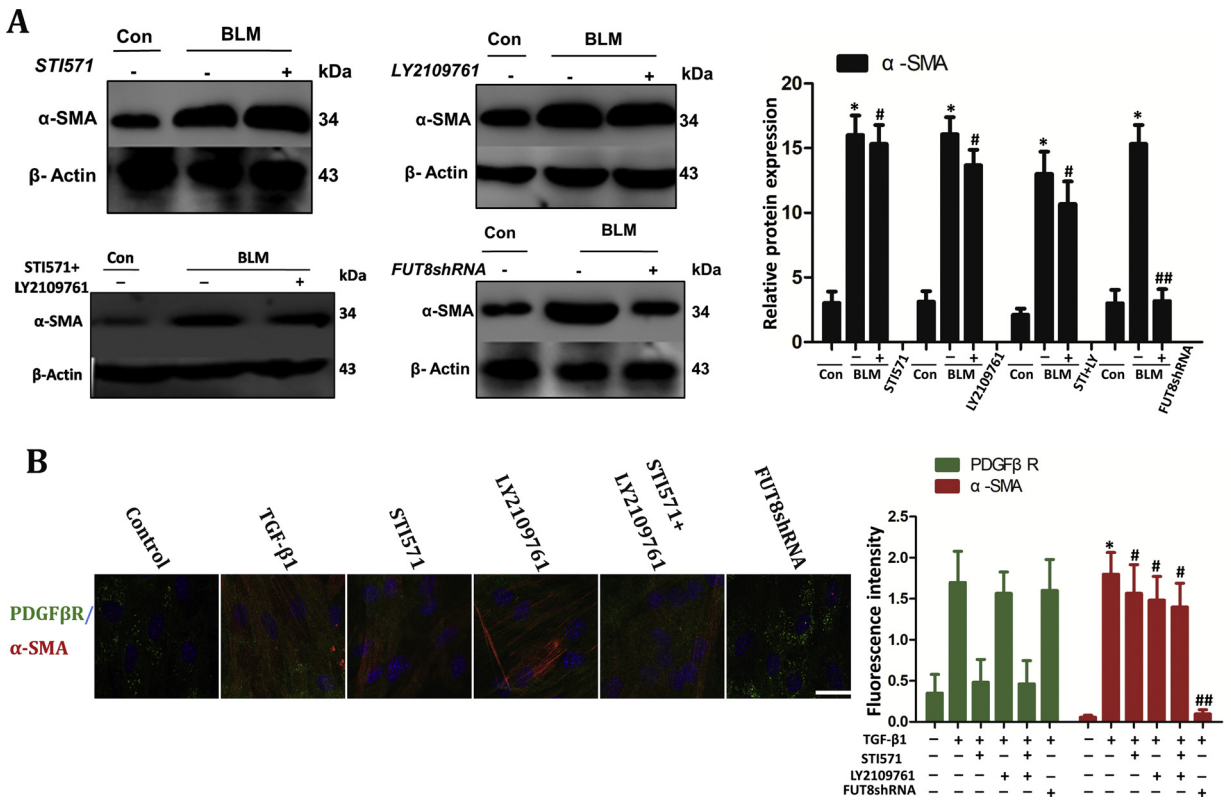

Fig. 4. *FUT8*shRNA inhibited pulmonary pericyte-myofibroblast transition. A: α-SMA expression in the pulmonary mesenchyme of each group by Western blot and quantitative analysis. B: PDGFβR and α-SMA expression in the pericytes of each group by immunofluorescence and quantitative analysis. *P < 0.01 versus Control group; #P > 0.05 versus TGF-β1 group; ##P < 0.01 versus TGF-β1 group. Scale bar: 50 μm. All data are expressed as the mean ± S.D. values. Each experiment was repeated three times (n = 6).

3.4. The effect of FUT8shRNA, STI571, and LY2109761 on pulmonary pathology and ECM in a BLM model

In general, the lung tissue lost its original morphological structure 28 days following BLM administration. After ST1571 and LY21079761 in the BLM model of pulmonary fibrosis, lung pathology was moderately alleviated. However, the degree of fibrosis in the *FUT8*shRNA group was significantly reduced, which was greater than treatment with ST1571 and LY2109761 (Fig. 5A). Collagen I and Collagen III are important components of the ECM (Zuo et al., 2017). MMP9 is involved in the decomposition of extracellular matrix. TIMP-1 is an inhibitor of ECM degrading enzymes (Hu et al., 2017). We used immunohistochemical methods to detect the expression of Collagen I, Collagen III, TIMP-1 and MMP9. The results showed that *FUT8*shRNA can obviously decrease the expression of Collagen I, Collagen III, and TIMP-1, While elevated the expression of MMP9 and the effect was substantially greater than the ST1571 and LY2109761 groups (Fig. 5B). These findings indicate that CF modification catalyzed by FUT8 may be a novel therapeutic target for pulmonary fibrosis.

3.5. Modification characteristics of CF catalyzed by FUT8 in pericyte transdifferentiation

We further detected whether FUT8-catalyzed CF modification was accompanied by pericyte transdifferentiation. After incubating pericytes with TGF-β1 for 48 h, the expression of the green fluorescently labeled FUT8 and red fluorescently labeled α-SMA increased substantially compared with the control group. After inhibiting CF modification with FUT8shRNA, the fluorescent intensity of FUT8 and α-SMA decreased significantly (Fig. 6A). The double immunofluorescence staining and Western blot analysis revealed that 28 days after BLM administration, the expression of FUT8 and α-SMA were obviously up-regulated in the pulmonary mesenchyme compared with the control group. FUT8shRNA can obviously reverse the expression of α-SMA and FUT8 in the pulmonary mesenchyme (Fig. 6B and C). These results indicate that FUT8 is associated with expression of α-SMA, including pericyte transdifferentiation.

3.6. Inhibition of CF modification via FUT8shRNA-mediated blockade of the PDGFβ/pErk and TGF-β/pSmad2/3 signaling pathways

Our previous studies confirmed that PDGFβR and TGFβR are modified by CF and the effects of fucosylation of TGFβR and PDGFβR on pulmonary fibrosis are independent of their protein expression levels (Sun et al., 2017). Therefore, whether *FUT8*shRNA inhibits CF modification and the activation of multiple signaling pathways at the same time. After incubating pericytes with TGF-β1 for 48 h in vitro, the expression of p-Erk and p-Smad2/3 were substantially up-regulated (Fig. 7A). At the same time, FUT8shRNA inhibited the substantial downregulation of p-Erk and p-Smad2/3 expression in the pulmonary mesenchyme compared with the BLM group (Fig. 7B and C). The results indicated that FUT8shRNA blocks the activation of multiple signaling pathways by inhibiting CF modification.

4. Discussion

The present findings support the reported evidence that pericytes are a substantial source of myofibroblasts, which is the direct cause of pulmonary fibrosis (Hu et al., 2017; Zhao et al., 2017; Barron et al., 2016; Wang et al., 2019a, 2019b). Inhibition of pericytes to myofibroblasts may be a significant target for pulmonary fibrosis. Moreover, our study found that blocking CF can inhibit pericyte activation and lung fibrosis.

Pericyte regulatory mechanisms are unclear. A complex interactive

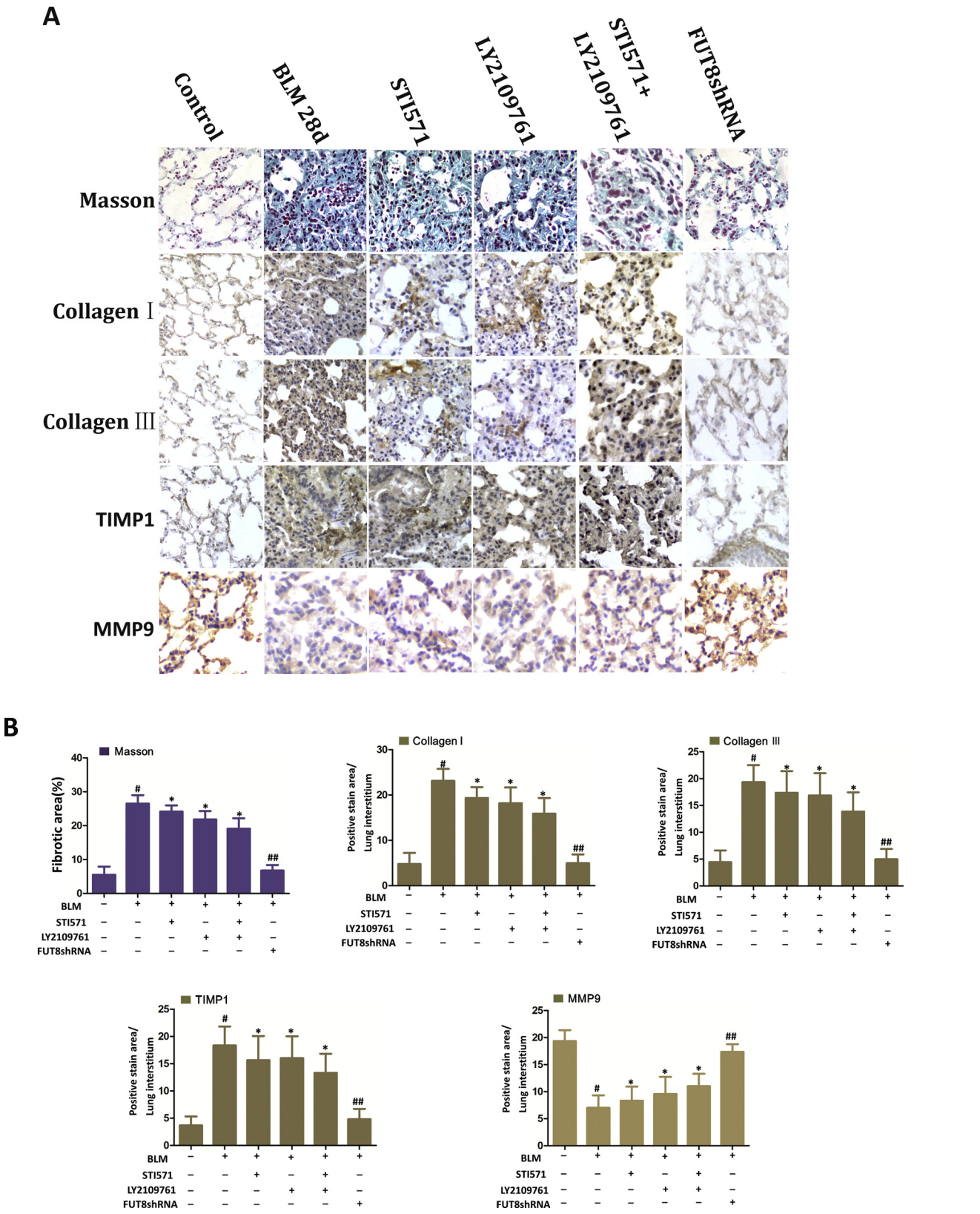

Fig. 5. *FUT8*shRNA, STI571, and LY2109761 treatment decreased pulmonary fibrosis in a BLM model. A: Masson staining and immunohistochemical examination. B: computer-based morphometric analysis of pulmonary fibrosis in each group; #P < 0.01 versus Control group; *P > 0.05 versus BLM group; ##P < 0.01 versus BLM group.Each experiment was repeated three times. Magnification: × 400.

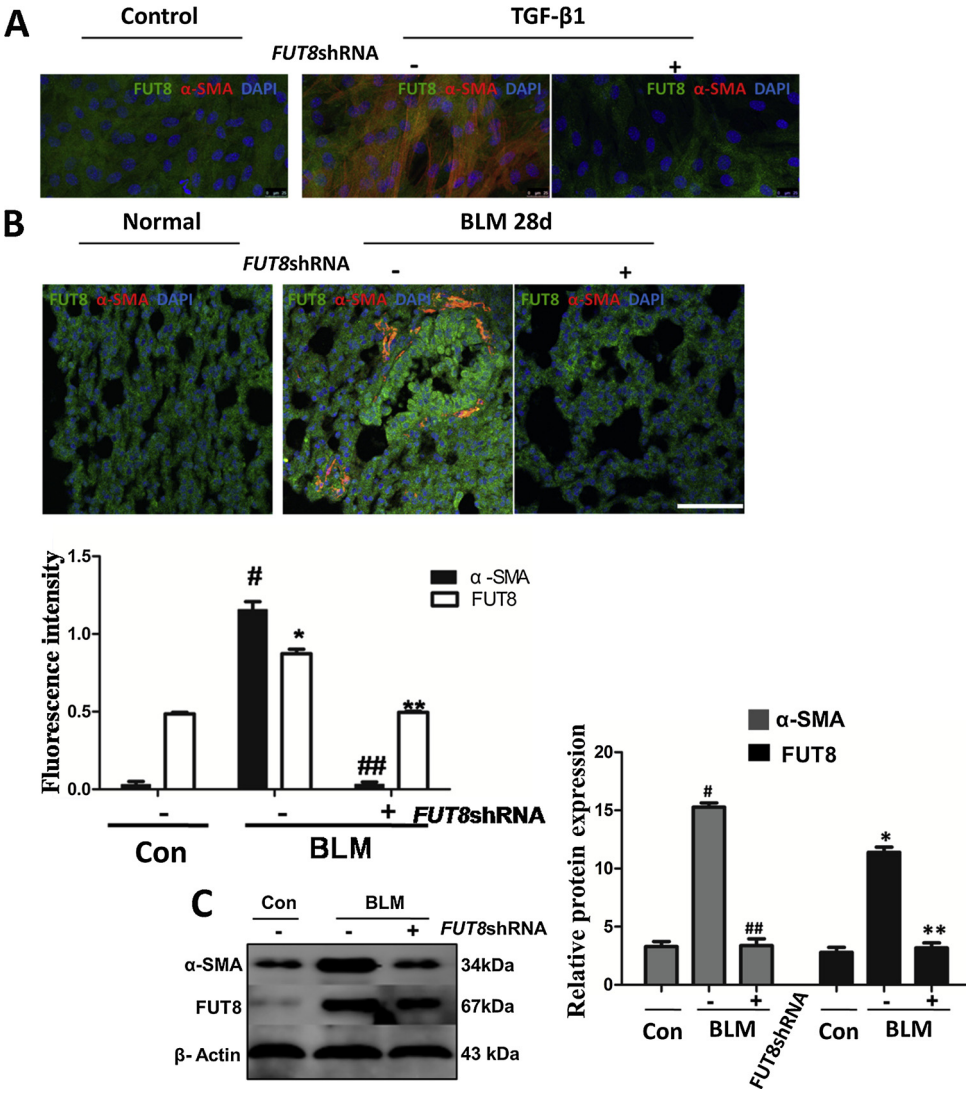

Fig. 6. Expression change of FUT8, α-SMA before and after pericyte transition. A and B: Change in FUT8 and α-SMA protein expression in vitro and in vivo by double immunofluorescent and quantitative analysis. C: Change in the expression of FUT8 and α-SMA protein in the pulmonary mesenchyme of each group by Western blot and quantitative analysis. All the data are expressed as the mean ± S.D. values. Scale bar: 50 μm. *P < 0.01 #P < 0.01 versus the Control group. **P < 0.01 ##P < 0.01 versus the BLM group. Each experiment was repeated for three times (n = 6).

network of signaling pathways exist between pericytes and endothelial cells, such as TGF-β, PDGF (Yamamizu et al., 2017; Shah and Kang, 2018). This study also found that FUT8, PDGFβR, and TGFβR are key proteins in pericyte activation (Fig. 1). Blocking the activation of a single signaling pathway may not be sufficient to inhibit the development of pulmonary fibrosis.

In our study, we used small molecule receptor antagonists, ST1571 and LY2109761 to block the activation of the PDGFβR and TGFβR, and observed the ability of the pericytes to myofibroblasts. (Fig. 2). As an important means of post-translational modification, glycosylation plays an essential role in protein functionality (e.g., the recognition of ligands) (Gloster and Vocadlo, 2012; Chen et al., 2013; Wang et al., 2006). Our previous studies have found that PDGFβR and TGFβR are glycoproteins modified by CF catalyzed by FUT8 (Sun et al., 2017). Therefore, we hope to treat FUT8 as a common target for the intervention of multiple signaling pathways.

Pericytes do not have specific markers, their diverse characteristics indicate that they have the capacity to easily differentiate (Rustenhoven et al., 2016; Siedlecki et al., 2017). In our study, we used PDGFβR, Desmin, and α-SMA to label pericytes. Consistent with previous reports, we found that pericytes detached from endothelial cells and transdifferentiated to myofibroblasts in primary cultured pericytes and a BLM-induced mouse model (Figs. 3 and 4). This study revealed that treatment with ST1571 and LY2109761 were unable to completely block the detachment and transdifferentiation of activated pericytes. In the *FUT8*shRNA group, the total number of pericytes (PDGFβR+, α-SMA+, and Desmin+) in the pulmonary mesenchyme substantially decreased (Fig. 3). These results indicate that pericyte activation was regulated by multiple signaling pathways. A single pathway inhibitor may be insufficient to inhibit pericyte activation. Therefore, CF has been shown to an important regulator in pericyte activation.

There are reports in the literature that FUT8 can catalyze CF modification of surface antigen, receptor, and adhesion molecules (Li et al., 2019). The small molecular receptor antagonists, STI571 and LY2109761, can neither decrease the collagen fibers nor reverse the destruction of the lung (Fig. 5A and B). However, we used *FUT8*shRNA, which inhibited multiple signaling pathways by down-regulating CF modification in the lungs, resulting in an obvious improvement in lung fibrosis and pulmonary structure (Fig. 5). It is important to note that *FUT8*shRNA improves the extent of lung pathology via inhibiting the activation of the PDGF and TGF-β pathways, as well as FUT8-mediated regulation of multiple proteins in pulmonary fibrosis.

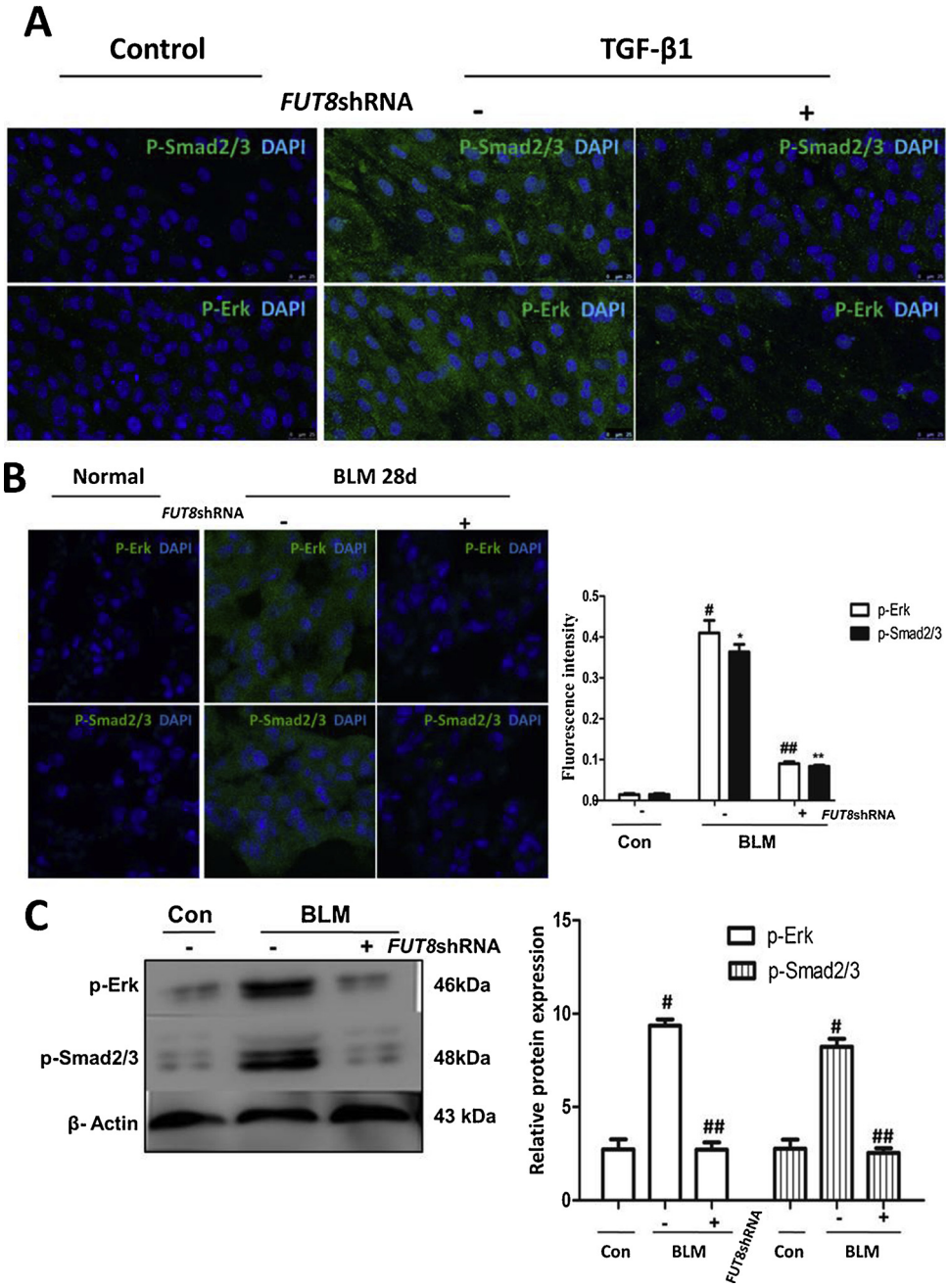

Fig. 7. FUT8shRNA inhibited the expression of downstream phosphorylated proteins p-Erk and p-Smad2/3. A and B: p-Erk and p-Smad2/3 in the pulmonary pericytes were detected in vitro and in vivo by immunofluorescent staining and quantitative analysis. C: p-Erk and p-Smad2/3 protein in the pulmonary mesenchyme of each group by Western blot and quantitative analysis. Scale bar: 50 μm. *P < 0.01 #P < 0.01 versus the control group; **P < 0.01 ##P < 0.01versus BLM group. All the data are expressed as the mean ± S.D. values. Each experiment was repeated three times (n = 6).

In the present study, we observed up-regulated FUT8 expression in association with the pericyte transition process (Fig. 6). Moreover, silencing FUT8 expression was shown to inhibit the transdifferentiation of pericytes into myofibroblasts. Taken together, these results indicate that the CF modification catalyzed by FUT8 may affect cell types other than pericytes.

Cross-talk between the TGF-β and PDGF signalling pathways are commonly found between endothelial cells and pericytes (Yamamizu et al., 2017). TGF-β1 signaling induces the phosphorylation of Smad2/3 proteins, which controls the expression in fbrogenic genes (Shah and Kang, 2018). PDGF signaling was reported to stimulate ERK1/2 activation in pericytes (Shah et al., 2018). Both the TGF-β/Smad and PDGF/ERK pathways were activated following BLM inducd pulmonary fibrosis in mice (Zhao et al., 2017). Moreover, our previous studies confirmed that CF has been shown to affect the binding of receptors (TGFβR and PDGFβR) and associated ligands (Sun et al., 2017). This finding indicates that *FUT8*shRNA inhibits pericyte activation by inhibiting the expression of downstream phosphorylated proteins involved in multiple signaling pathways (Fig. 7).

FUT8 plays an important regulatory role in the transdifferentiation of pericytes into myofibroblasts, providing a potential “hub” target for the treatment of pulmonary fibrosis. Due to the limitations of experimental techniques, FUT8 expression in *FUT8*shRNA silenced mice is not as accurate as that of conditional knockout mice, which require further study.

5. Conclusions

Our findings demonstrate that blocking CF in pericytes is more effective at preventing the transformation of these cells than small molecule inhibitors targeting the TGFβ and PDGFβR signaling pathways. In addition, there is a causal relationship between CF modification catalyzed by FUT8 and pulmonary fibrosis. Our findings suggest that FUT8 may be a novel therapeutic target for pulmonary fibrosis.

Declaration of Competing Interest

All the authors declared that they have no conflicts of interest to this work.

Acknowledgements

Ying Sun and Wei Sun are sharing the first authorship. Ning Yang, Ying Sun, Haiying Tang and Fengzhou Li performed the research; Taihua Wu, Hongli Lin and Wei Sun designed the study; Lili Gao, Xiuna Sun, Jia Liu, Fuyang Pei and Jia Liu analyzed the data; Taihua Wu, Hongli Lin and Wei Sun wrote the paper. All authors read and approved the final manuscript.

Funding

This work was supported by the Key Program of National Natural Science Foundation of China (NSFC) [grant numbers 81670063 to TW, 81530021 to HL)] and Research Fund for the Doctoral Program of Higher Education of China [grant number 20132015110003 to HL].

References

Barron, L., Gharib, S.A., Duffield, J.S., 2016. Lung pericytes and resident fibroblasts: busy multitaskers. Am. J. Pathol. 186, 2519–2531.

Braun, R.K., Broytman, O., Braun, F.M., Brinkman, J.A., Clithero, A., Modi, D., Pegelow, D.F., Eldridge, M., Teodorescu, M., 2018. Chronic intermittent hypoxia worsens bleomycin-induced lung fibrosis in rats. Respir. Physiol. Neurobiol. 256, 97–108.

Castellano, G., Stasi, A., Franzin, R., Sallustio, F., Divella, C., Spinelli, A., Netti, G.S., Fiaccadori, E., Cantaluppi, V., Crovace, A., et al., 2019. LPS-binding protein modulates acute renal fibrosis by inducing pericyte-to-Myofibroblast trans-differentiation through TLR-4 signaling. Int. J. Mol. Sci. 27, 3682.

Chen, C.Y., Jan, Y.H., Juan, Y.H., Yang, C.J., Huang, M.S., Yu, C.J., Yang, P.C., Hsiao, M., Hsu, T.L., Wong, C.H., 2013. Fucosyltransferase 8 as a functional regulator of non-small cell lung cancer. Proc. Natl. Acad. Sci. U. S. A. 110, 630–635.

Chen, Y.H., Chen, C.L., Lu, D.W., Liang, C.M., Tai, M.C., Chen, J.T., 2016. Silibinin inhibits platelet-derived growth factor-driven cell proliferation via downregulation of N-Glycosylation in human tenon's fibroblasts in a proteasome-dependent manner. PLoS One 11, e0168765.

Feng, F., Zhang, J., Wang, Z., Wu, Q., Zhou, X., 2019. Efficacy and safety of *N*-acetylcysteinetherapyfor idiopathicpulmonary fibrosis: an updated systematic review and meta-analysis. Exp. Ther. Med. 18, 802–816.

Gloster, T.M., Vocadlo, D.J., 2012. Developing inhibitors of glycan processing enzymes as tools for enabling glycobiology. Nat. Chem. Biol. 8, 683–694.

Hirano, M., Totani, K., Fukuda, T., Gu, J., Suzuki, A., 2017. N-Glycoform-dependent interactions of megalin with its ligands. Biochim. Biophys. Acta 1861, 3106–3118.

Hirooka, T., Yoshida, E., Eto, K., Kaji, T., 2017. Methylmercury induces hyaluronan synthesis in cultured human brain microvascular endothelial cells and pericytes via different mechanisms. J. Toxicol. Sci. 42, 329–333.

Hu, X., Fernandes, J., Jones, D.P., Go, Y.M., 2017. Cadmium stimulates myofibroblast differentiation and mouse lung fibrosis. Toxicology 383, 50–56.

Kathiriya, J.J., Nakra, N., Nixon, J., Patel, P.S., Vaghasiya, V., Alhassani, A., Tian, Z., Allen-Gipson, D., Davé, V., 2017. Galectin-1 inhibition attenuates profibrotic signaling in hypoxia-induced pulmonary fibrosis. Cell Death Discov. 3, 17010.

Kumar, A., D'Souza, S.S., Moskvin, O.V., Toh, H., Wang, B., Zhang, J., Swanson, S., Guo, L.W., Thomson, J.A., Slukvin, I.I., 2017. Specification and diversification of pericytes and smooth muscle cells from Mesenchymoangioblasts. Cell Rep. 19, 1902–1916.

Li, M., Bai, Y., Zhou, J., Huang, W., Yan, J., Tao, J., Fan, Q., Liu, Y., Mei, D., Yan, Q., et al., 2019. Core fucosylation of maternal milk N-Glycan evokes B cell activation by selectively promoting the l-Fucose metabolism of gut Bifidobacterium spp and Lactobacillus spp. MBio. 10, e00128–19.

Lunardi, F., Pezzuto, F., Vuljan, S.E., Calabrese, F., 2018. Idiopathic pulmonary fibrosis and antifibrotic treatments: focus on experimental studies. Arch. Pathol. Lab. Med. 142, 1090–1097.

Minutti, C.M., Modak, R.V., Macdonald, F., Li, F., Smyth, D.J., Dorward, D.A., Blair, N., Husovsky, C., Muir, A., Giampazolias, E., et al., 2019. Activation of the Wnt/planar cell polarity pathway is required for pericyte recruitment during pulmonary angiogenesis. Immunity 50, 645–654.

Pozdzik, A.A., Giordano, L., Li, G., Antoine, M.H., Quellard, N., Godet, J., De, P., Husson, C., Declèves, A.E., Arlt, V.M., et al., 2016. Blocking TGF-β signaling pathway preserves mitochondrial proteostasis and reduces early activation of PDGFRβ+ pericytes in aristolochic acid induced acute kidney injury in wistar male rats. PLoS One 11, e0157288.

Rustenhoven, J., Aalderink, M., Scotter, E.L., Oldfield, R.L., Bergin, P.S., Mee, E.W., Graham, E.S., Faull, R.L., Curtis, M.A., Park, T.I., et al., 2016. TGF-beta1 regulates human brain pericyte inflammatory processes involved in neurovasculature function. J. Neuroinflammation 13, 37.

Sava, P., Ramanathan, A., Dobronyi, A., Peng, X., Sun, H., Ledesma-Mendoza, A., Herzog, E.L., Gonzalez, A.L., 2017. Human pericytes adopt myofibroblast properties in the microenvironment of the IPF lung. JCI Insight 2.

Shao, S., Zhang, X., Duan, L., Fang, H., Rao, S., Liu, W., Guo, B., Zhang, X., 2018. Lysyl hydroxylase inhibition by minoxidil blocks collagen deposition and prevents pulmonary fibrosis via TGF-β_1/Smad3 signaling pathway. Med. Sci. Monit. 24, 8592–8601.

Shah, S., Kang, K.T., 2018. Two-cell spheroid angiogenesis assay system using both endothelial colony forming cells and mesenchymal stem cells. Biomol. Ther(Seoul). 26, 474–480.

Shen, N., Lin, H., Wu, T., Wang, D., Wang, W., Xie, H., Zhang, J., Feng, Z., 2013. Inhibition of TGF-β1-receptor posttranslational core fucosylation attenuates rat renal interstitial fibrosis. Kidney Int. 84, 64–77.

Siedlecki, J., Wertheimer, C., Wolf, A., Liegl, R., Priglinger, C., Priglinger, S., Eibl-Lindner, K., 2017. Combined VEGF and PDGF inhibition for neovascular AMD: anti-angiogenic properties of axitinib on human endothelial cells and pericytes in vitro. Graefes Arch. Clin. Exp. Ophthalmol. 255, 963–972.

Sköld, C.M., Arnheim-Dahlström, L., Bartle, K., Janson, C., Kirchgaessler, K.U., Levine, A., Ferrara, G., 2019. Patient journey and treatment patterns in adults with IPF based on health care data in Sweden from 2001 to 2015. Respir. Med. 155, 72–78.

Starling, S., 2017. Renal fibrosis: pericytes activate complement in fibrosis. Nat. Rev. Nephrol. 13, 262.

Sun, W., Tang, H., Gao, L., Sun, X., Liu, J., Wang, W., Wu, T., Lin, H., 2017. Mechanisms of pulmonary fibrosis induced by core fucosylation in pericytes. Int. J. Biochem. Cell Biol. 88, 44–54.

Terashima, H., Aonuma, M., Tsuchida, H., Sugimoto, K., Yokoyama, M., Kato, M., 2019. Ttenuation of pulmonary fibrosis in type I collagen-targeted reporter mice with ALK-5 inhibitors. Pulm. Pharmacol. Ther. 54, 31–38.

Underly, R.G., Levy, M., Hartmann, D.A., Grant, R.I., Watson, A.N., Shih, A.Y., 2017. Pericytes as inducers of rapid, matrix Metalloproteinase-9-Dependent capillary damage during ischemia. J. Neurosci. 37, 129–140.

Urushiyama, H., Terasaki, Y., Nagasaka, S., Kokuho, N., Endo, Y., Terasaki, M., Kunugi, S., Makita, K., Isago, H., Hosoki, K., et al., 2019. Naftopidil reduced the proliferation of lung fibroblasts and bleomycin-induced lung fibrosis in mice. J. Cell. Mol. Med. 23, 3563–3571.

Wang, L., Zhang, P., Li, X., Zhang, Y., Zhan, Q., Wang, C., 2019a. Low-molecular-weight fucoidan attenuates bleomycin-induced pulmonary fibrosis: possible role in inhibiting TGF-β1-induced epithelial-mesenchymal transition through ERK pathway. Am. J. Transl. Res. 11, 2590–2602.

Wang, S., Zaitoun, I.S., Johnson, R.P., Jamali, N., Gurel, Z., Wintheiser, C.M., Strasser, A., Lindner, V., Sheibani, N., Sorenson, C.M., 2017. Bim expression in endothelial cells and pericytes is essential for regression of the fetal ocular vasculature. PLoS One 12, e0178198.

Wang, X., Gu, J., Miyoshi, E., Honke, K., Taniguchi, N., 2006. Phenotype changes of Fut8 knockout mouse: core fucosylation is crucial for the function of growth factor receptor(s). Methods. Enzymol. 417, 11–22.

Wang, Y.C., Chen, Q., Luo, J.M., Nie, J., Meng, Q.H., Shuai, W., Xie, H., Xia, J.M., Wang, H., 2019b. Notch1 promotes the pericyte-myofibroblast transition in idiopathic pulmonary fibrosis through the PDGFR/ROCK1 signal pathway. Exp. Mol. Med. 51, 35.

Yamamizu, K., Iwasaki, M., Takakubo, H., Sakamoto, T., Ikuno, T., Miyoshi, M., Kondo, T., Nakao, Y., Nakagawa, M., Inoue, H., et al., 2017. In vitro administration of blood-brain barrier with human iPSC-Derived endothelial cells, pericytes, neurons, and astrocytes via notch signaling. Stem Cell Reports 10, 634–647.

Zhao, B., Guan, H., Liu, J.Q., Zheng, Z., Zhou, Q., Zhang, J., Su, L.L., Hu, D.H., 2017. Hypoxia drives the transition of human dermal fibroblasts to a myofibroblast-like phenotype via the TGF-β1/Smad3 pathway. Int. J. Mol. Med. 39, 153–159.

Zuo, W.L., Zhao, J.M., Huang, J.X., Zhou, W., Lei, Z.H., Huang, Y.M., Huang, Y.F., Li, H.G., 2017. Effect of bosentan is correlated with MMP-9/TIMP-1 ratio in bleomycin-induced pulmonary fibrosis. Biomed. Rep. 6, 201–205.